AFRL-RV-HA-
TR-2010-1117

AFRL-RV-HA-
TR-2010-1117

SPACE PARTICLE MODELING, MEASUREMENTS AND EFFECTS: COMPACT ENVIRONMENTAL ANOMALY SENSOR (CEASE) PROTON CALIBRATION

Bronislaw K. Dichter, et al.

Assurance Technology Corporation
84 South Street
Carlisle, MA 01741-1515

7 February 2011

Interim Report

APPROVED FOR PUBLIC RELEASE; DISTRIBUTION IS UNLIMITED

AIR FORCE RESEARCH LABORATORY
Space Vehicles Directorate
29 Randolph Rd.
AIR FORCE MATERIEL COMMAND
HANSCOM AFB, MA 01731-3010

DTIC COPY

NOTICE AND SIGNATURE PAGE

AFRL-RV-HA-TR-2010-1117 HAS BEEN REVIEWED AND IS APPROVED FOR PUBLICATION IN ACCORDANCE WITH ASSIGNED DISTRIBUTION STATEMENT.

//Signed//	//Signed//
Chadwick Lindstrom, PhD	Joel Mozer, PhD
Program Manager	Chief, AFRL/RVB

REPORT DOCUMENTATION PAGE	*Form Approved* *OMB No. 0704-0188*

1. REPORT DATE *(DD-MM-YYYY)* 07-02-2011	**2. REPORT TYPE** Interim Report	**3. DATES COVERED** *(From - To)* 03-01-2009 To 28-02-2010

4. TITLE AND SUBTITLE Space Particle Modeling, Measurements, and Effects: Compact Environmental Anomaly Sensor (CEASE) Proton Calibration	**5a. CONTRACT NUMBER** FA8718-08-C-0017 **5b. GRANT NUMBER** **5c. PROGRAM ELEMENT NUMBER** 63401F
6. AUTHOR(S) Bronislaw K. Dichter, Edward G. Mullen, Gary E. Galica	**5d. PROJECT NUMBER** 5021 **5e. TASK NUMBER** **5f. WORK UNIT NUMBER** 837121
7. PERFORMING ORGANIZATION NAME(S) AND ADDRESS(ES) Assurance Technology Corporation 84 South Street Carlisle, MA 01741-1515	**8. PERFORMING ORGANIZATION REPORT NUMBER**
9. SPONSORING / MONITORING AGENCY NAME(S) AND ADDRESS(ES) Air Force Research Laboratory Space Vehicles Directorate 29 Randolph Road Hanscom AFB, MA 01731-3010	**10. SPONSOR/MONITOR'S ACRONYM(S)** AFRL/RVBXR **11. SPONSOR/MONITOR'S REPORT NUMBER(S)** AFRL-RV-HA-TR-2010-1117

12. DISTRIBUTION / AVAILABILITY STATEMENT

Approved for public release; distribution is unlimited. 377ABW-2011-0051; 18 January 2011.

13. SUPPLEMENTARY NOTES

14. ABSTRACT

This report describes the first calibration of the Compact Environmental Anomaly Sensor (CEASE) instrument particle telescope with high energy (> 20 MeV) protons. The two units calibrated were S/N 004 (flight unit w/tungsten collimator) and S/N 006 (engineering unit identical to the Tri-Service Experiment 5 [TSX-5]) CEASE. Both instruments were calibrated at the cyclotron at the Francis H. Burr Proton Therapy Center at the Massachusetts General Hospital (MGH). We report the results of those calibrations and the subsequent analyses.

15. SUBJECT TERMS

Space Instrumentation, Electrons, Protons, High Energy

16. SECURITY CLASSIFICATION OF:			**17. LIMITATION OF ABSTRACT**	**18. NUMBER OF PAGES**	**19a. NAME OF RESPONSIBLE PERSON**
					Dr. Chadwick Lindstrom
a. REPORT UNCLASSIFIED	**b. ABSTRACT** UNCLASSIFIED	**c. THIS PAGE** UNCLASSIFIED	Unlimited	26	**19b. TELEPHONE NUMBER** *(include area code)*

Standard Form 298 (Rev. 8-98)
Prescribed by ANSI Std. Z39.18

This page is intentionally left blank.

TABLE OF CONTENTS

List of Figures

Figure **Page**

List of Tables

Table **Page**

This page is intentionally left blank.

1. INTRODUCTION

This report describes research conducted in the area of development of enhanced particle measurement techniques and systems that provide smaller, lighter and higher performance capability instrumentation for measuring the space particle environment.

Specifically, we describe the first calibration of the Compact Environment Anomaly Sensor (CEASE) instrument particle telescope with high energy (> 20 MeV) protons. Two units were calibrated: S/N 004 is the flight unit for an upcoming mission; S/N 006 is an engineering unit identical to the CEASE unit flown on the Tri-Service Experiment Mission 5 (TSX-5). The primary difference between the two units was that the 5 mm thick telescope top was made from copper for S/N 006 and tungsten for S/N 004. Both instruments were calibrated with the proton cyclotron at the Francis H. Burr Proton Therapy Center at the Massachusetts General Hospital (MGH). We report the results of those calibrations.

2. BACKGROUND

2.1 Overview

Within the "Space Particle Modeling, Measurements and Effects" program, ATC performs research in three related fields: 1) Modeling of space particles for improved monitoring, forecasting and space systems design, 2) Developing of enhanced particle measurement techniques and systems to provide smaller, lighter and higher performance capability instrumentation, and 3) Relation of space particle populations and dynamics to space system anomalies and space assets degradation and/or outages The three research areas are interrelated as they all pertain to elements needed to provide a clear understanding of near-Earth particle dynamics and their impact on USAF assets/operations.

The work described herein falls within Area 2. We have applied enhanced-performance particle measurement and sensor calibration technologies developed by ATC for other space particle instrumentation to USAF specific requirements for smaller, lighter, higher performance instrumentation. We have tested prototype space subsystems/circuits/sensor elements to demonstrate the applicability of the enhanced techniques and technologies. And we have provided integration support for space instrumentation as needed to ensure proper operation of instruments and quality of the data gathered.

The project team comprises ATC personnel and expert consultants. The team combines the heritage, innovative approaches, centralized control and program flexibility of ATC with the expert knowledge of consultants selected for their leading edge research in the areas of space instrumentation and spacecraft anomaly investigations. Areas of expertise of the key team members are highlighted in Table 1.

Table 1 Key Team Members Expertise and Qualifications

Name	Company	Position	Program Area	Education/ Experience (Yrs)	Areas of Expertise
Galica, Gary	ATC	Senior Scientist	Program Manager, Data Modeling and Analyses	PhD Physical Chemistry / 20 Yrs	Program Management, Space Instrumentation & Data Analyses
McGarity, John	ATC	Senior Engineer	Sensor Design & Development Eng.	BS EE / 25 Yrs	Miniature Sensor Concepts, Designs & Development – SSJ5, CEASE I & II, SPREE, etc
Fisher, Brian	ATC	Scientist	Modeling	PhD Physics / 5 Yrs	GEANT 4 Modeling, Instrument Design & Development, Space Data Analyses
Dichter, Bronek	ATC	Senior Scientist	Space Instrumentation	PhD Physics / 20 Yrs	Space instrumentation Design, Development & Test
Mullen, Gary	ATC	Vice President	Program Manager & Lead Program Scientist	BS Physics / 30 Yrs	Space Effects, Space Sensor Systems, Anomaly Analyses & Tiger Team Participant
Hanser, Fred	ATC	Senior Scientist	System Design	PhD Physics / 30 Yrs	Instrument Design & Test Physicist For Space Particle Instruments Including GOES, POES, SCATHA, DMSP, etc.

2.2 CEASE Instrument Description

CEASE has four sensors for measuring the space particle environment: a particle telescope, two dosimeters, and a Single Event Effects (SEE) detector. Telescope provides the energy distributions and fluxes of protons and electrons in the local environment. The calibrations described here were performed on the CEASE particle telescope. The dosimeters determine the total ionizing dose behind shield of two difference thicknesses: 0.080 inches and 0.25 inches of aluminum. These two thicknesses correspond to the amount of effective aluminum protection for lightly and highly shielded electronic components. The SEE detector is a photodiode configuration identical to the dosimeters but with a firing threshold set very high so only proton induced nuclear interactions and the passage of cosmic rays can trigger it. These events are counted so as to provide the local flux of SEE causing particles.

The energetic particle telescope consists of two coaxially mounted circular solid-state silicon sensors, a nominal 50 mm^2 area 150 μm thick front detector (DFT) and a nominal 85 mm^2 area 500 μm thick back detector (DBT). The detectors are located inside a copper enclosure which absorbs protons with $E < 60$ MeV and electrons with $E < 8$ MeV (see Figure 1). A front collimator, 0.039 cm thick tungsten disc, has a small aperture and a field-of-view opening half angle of 31°. The aperture diameter is 0.062 cm. A 9 μm thick Al foil covers the aperture to make it light tight to protect DFT from damaging sunlight and to determine the low energy cut-offs for the telescope: 50 keV for electrons and 700 keV for protons.

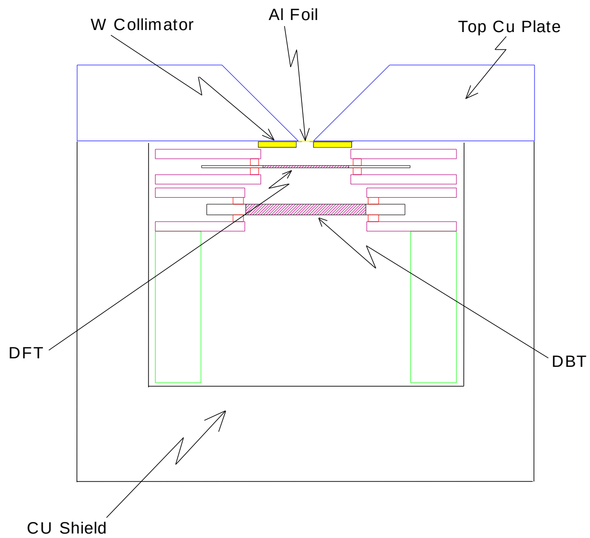

Figure 1 Cross Section Sketch of the Particle Telescope

The technique of particle type identification and energy measurement is accomplished by using the pattern of energy deposition in the telescope detectors. The output of each detector is connected to an eight-level threshold circuit that performs the pulse height analysis. In addition, DFT and DBT are also connected to a coincidence circuit with a 0.5 μsec resolving time. For a full description of the instrument and its data processing algorithms see Dichter *et al*. [1] and Brautigam [2].

3. TECHNICAL APPROACH

The telescope is calibrated by exposing the telescope front end to a beam of high energy protons and measuring its response while, simultaneously, measuring the beam flux. The diagram of the experimental configuration is shown in Figure 2. CEASE was mounted to a rotary fixture so that it could be rotated to any angle with respect to the beam. MON1 (M1) and MON2 (M2) are silicon solid state detectors used to determine the beam intensity changes during the measurement. MON1 had an 85 mm^2 area and was mounted at the same height as the CEASE telescope aperture but 1.52 cm to the side. MON2 had a 50 mm^2 area and was mounted on same fixture and the same height as the CEASE telescope so that so that it could be moved to the exact location of the telescope front face, with the MON2 center in the same location as the center of the telescope collimator (aperture substitution). Typical experimental sequence consisted on measuring the absolute beam flux with MON2 in the aperture substitution location while recording MON1 counts. This procedure transfers the absolute beam flux calibration at the CEASE location to the MON1 telescope at its location to the side of the CEASE aperture. Once the beam intensity was determined, CEASE was put into the beam spot and its response, as a function of angle with respect to the beam axis, θ, and beam energy, E, was measured and normalized to the beam flux using MON1.

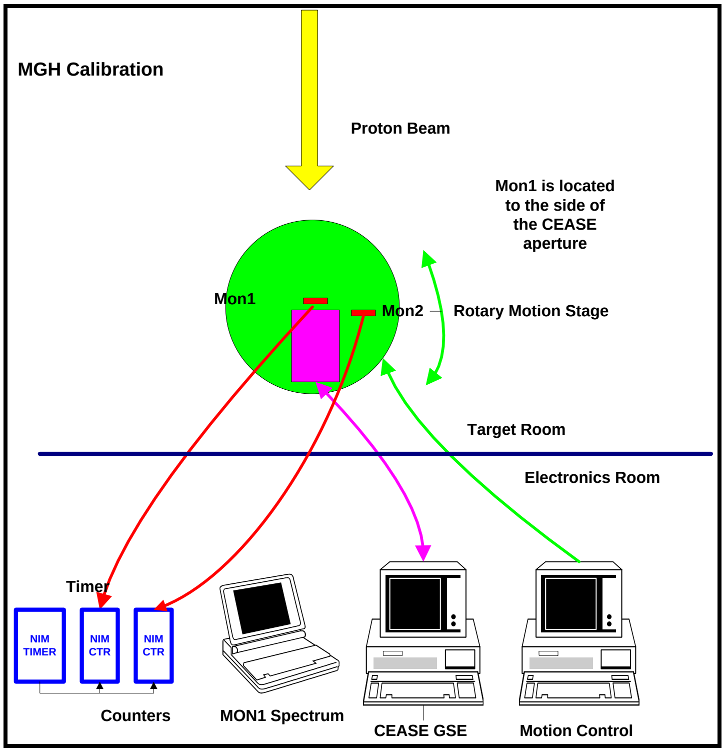

Figure 2 Experimental Configuration for the CEASE Calibrations

In terms of the algebra of the monitor count rates, the sequence can be expressed as follows. The absolute beam flux at the CEASE aperture location, F, is given by

$$F = \frac{C_2}{A_2 \Delta T} \tag{1}$$

where C_2 (C_1) are the M2 (M1) counts collected during a time interval ΔT and A_2 (A_1) is the detector area. During the M2 to M1 flux transfer time period, the ratio of the two count rates, R, is determined

$$R = \left[\frac{C_2}{C_1}\right] \tag{2}$$

Defining the off center flux, as measured by the M1 detector, analogously to the flux at the CEASE location, we can write

$$F = R\left[\frac{A_1}{A_2}\right]F_1 \tag{3}$$

The ratio of flux at the CEASE aperture location to the flux at the Mon1 location (F/F_1) for the S/N 004 runs in February and June 2009 is shown in Figure 3.

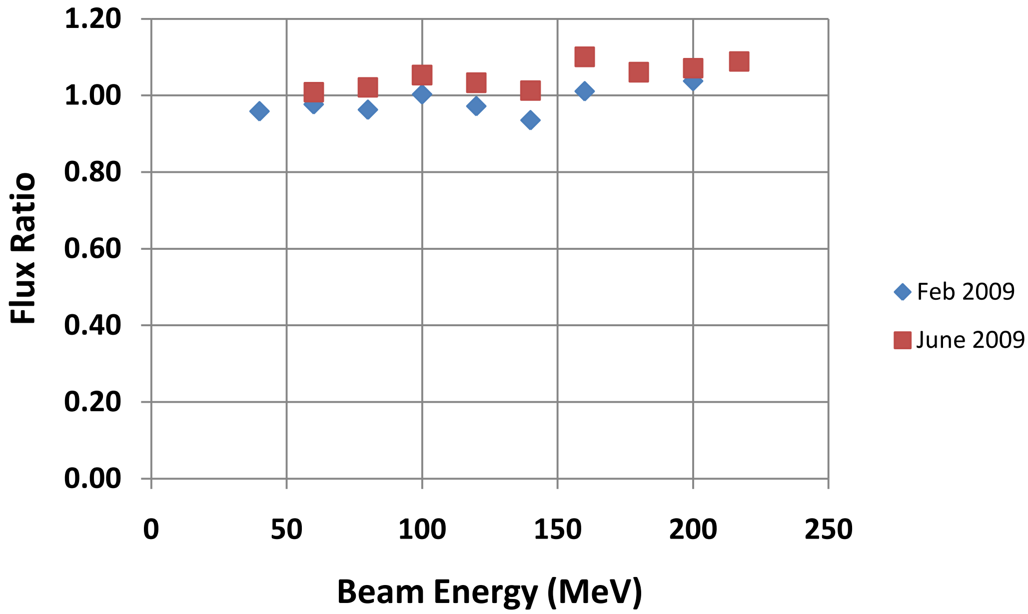

Figure 3 Ratio of Fluxes Measured by CEASE and the MON1 Detector

Except for the lowest beam energies, the beam spot is sufficiently large to be uniform over an area with a radius larger than the separation between Mon1 and Mon2. CEASE configuration for S/N 004 is described in Ref. 2, although the area of the front (DFT) and rear detectors (DBT) are treated differently in high energy proton calibrations. The nominal detector areas are 25 and 50 mm^2 but the known response to the particle adds approximately 1.2 mm to the detector radius. Since high energy protons can penetrate the telescope top cover, the effective DFT and DBT areas are close to 50 and 85 mm^2.

4. CEASE CALIBRATION RESULTS AND DISCUSSION

4.1 CEASE S/N 004 Calibration

The effective area for any CEASE channel T0n, as a function of proton angle of incidence, θ, and energy, E, is computed using the expression

$$A_{0n}(\theta, E) = \frac{C_{0n}(\theta, E)}{F\Delta T} \qquad (4)$$

where C_{0n} are the counts in the T0n channel. Substituting for F, as in eq. (3) and using the definition

$$F = R\left(\frac{A_1}{A_2}\right)F_1 = \frac{RC_1}{A_2\Delta T} \qquad (5)$$

yields

$$A_{0n}(\theta,E)=\frac{A_2 C_{0n}(\theta,E)}{RC_1(\theta,E)} \qquad (6)$$

The channel geometric factor, GF_{0n}, is defined by

$$GF_{0n}=2\pi\int A_{0n}(\theta,E)\sin(\theta)d\theta \qquad (7)$$

Effective 0^o areas (normal beam incidence) for the Tn channels are computed using eq. (6). The effective areas for normal beam incidence as a function of beam energy are listed in Table 2 and are plotted in Figure 4. The "All P" channel contains the sum of all CEASE particles not identified as electrons. The total effective area peaks at 0.379 cm^2 at 140 MeV. For energies above 140 MeV, proton counts begin to move out of the proton identification region into the electron region and effective area of the "All P" and sum of the Tn channels decreases with increasing proton energy.

Table 2 Measured Effective 0^o Areas for S/N 004 Proton Channels

Energy (MeV)	All P (cm^2)	T05 (cm)	T06 (cm^2)	T08 (cm^2)	T09 (cm^2)	Sum Tn (cm^2)
60	0.077	0.020	0.029	0.000	0.023	0.073
80	0.202	0.014	0.051	0.007	0.129	0.201
100	0.276	0.005	0.053	0.043	0.174	0.275
120	0.374	0.001	0.011	0.227	0.134	0.373
140	0.379	0.000	0.002	0.292	0.057	0.352
160	0.369	0.000	0.001	0.222	0.029	0.253
180	0.359	0.000	0.001	0.121	0.015	0.137
200	0.352	0.000	0.001	0.066	0.010	0.077
217	0.349	0.000	0.001	0.041	0.007	0.049

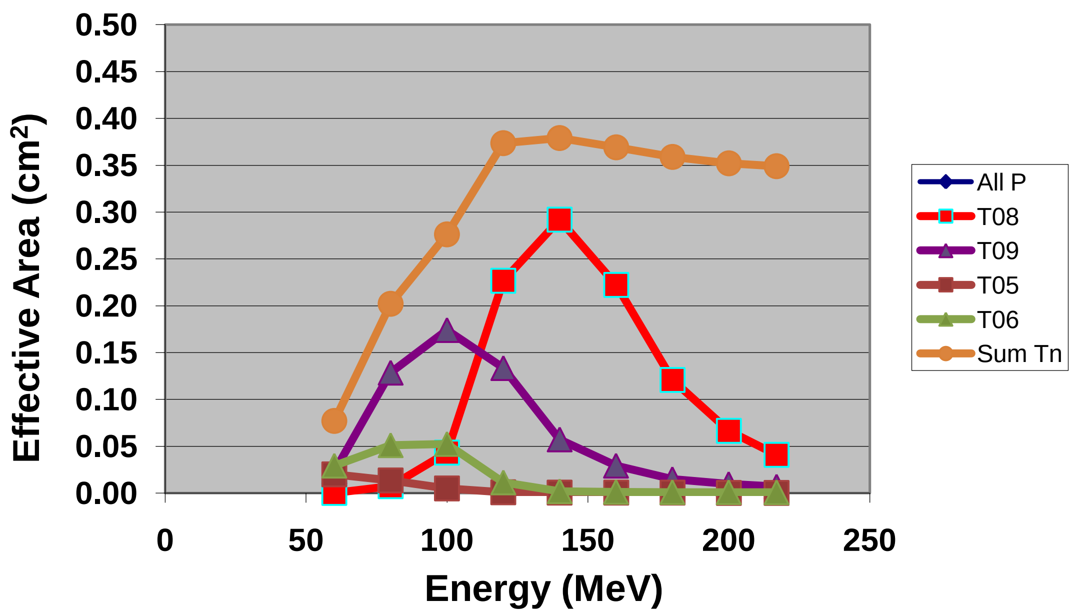

Figure 4 Measured Effective 0° Areas for S/N 004 Proton Channels

The geometric factors for S/N 004 Tn channels are listed in Table 3 and are plotted in Figure 5. Angular CEASE S/N 004 channel responses are tabulated in Tables 4 through 12.

Table 3 Measured Effective Geometric Factors for CEASE Proton Channels for S/N 004

E (MeV)	All Protons cm^2-sr	T05 cm^2-sr	T06 cm^2-sr	T08 cm^2-sr	T09 cm^2-sr	Sum Tn cm^2-sr
40	0.008	0.004	0.003	0.000	0.001	0.007
60	0.037	0.007	0.015	0.004	0.012	0.038
80	0.154	0.044	0.044	0.013	0.044	0.145
100	0.270	0.019	0.089	0.018	0.139	0.265
120	0.541	0.028	0.075	0.135	0.294	0.532
140	0.603	0.003	0.020	0.291	0.264	0.578
160	0.571	0.001	0.005	0.338	0.164	0.508
180	0.567	0.001	0.003	0.318	0.102	0.424
200	0.557	0.001	0.003	0.265	0.065	0.334
217	0.527	0.001	0.002	0.210	0.042	0.255

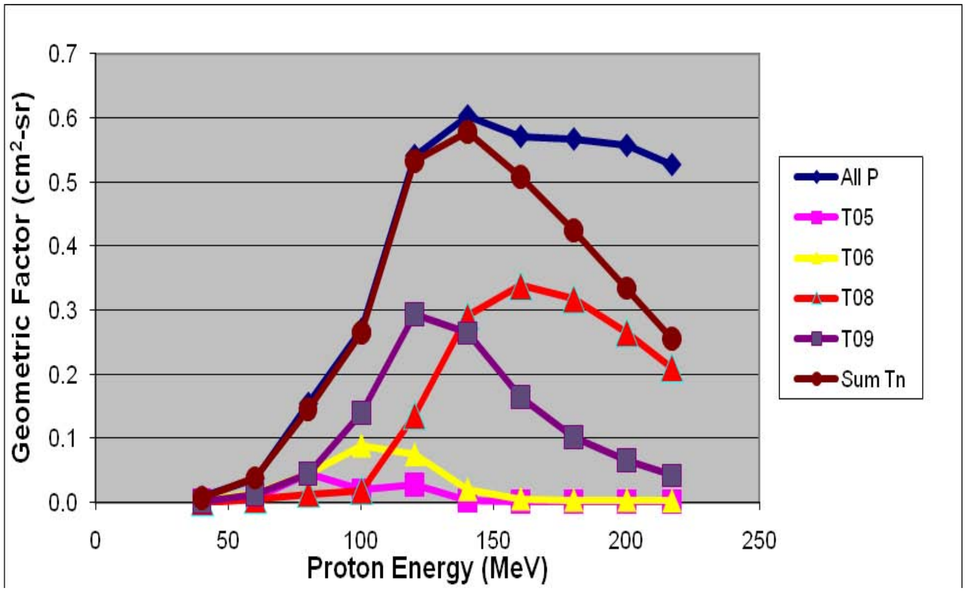

Figure 5 Measured Geometric Factors for S/N 004 Proton Channels

Comparison of results of GEANT calculations of the effective 0^o area to the measured values is shown in Figure 6. GEANT values have been scaled by 0.72. A scaling factor is needed because GEANT calculations assume an exact 0.5 cm^2 area detector (nominal radius of 2.8 mm plus an additional 1.2 mm) while the actual additional radius piece likely differs from 1.2 mm, by different amounts, for both the front telescope detector and the beam monitor detector.

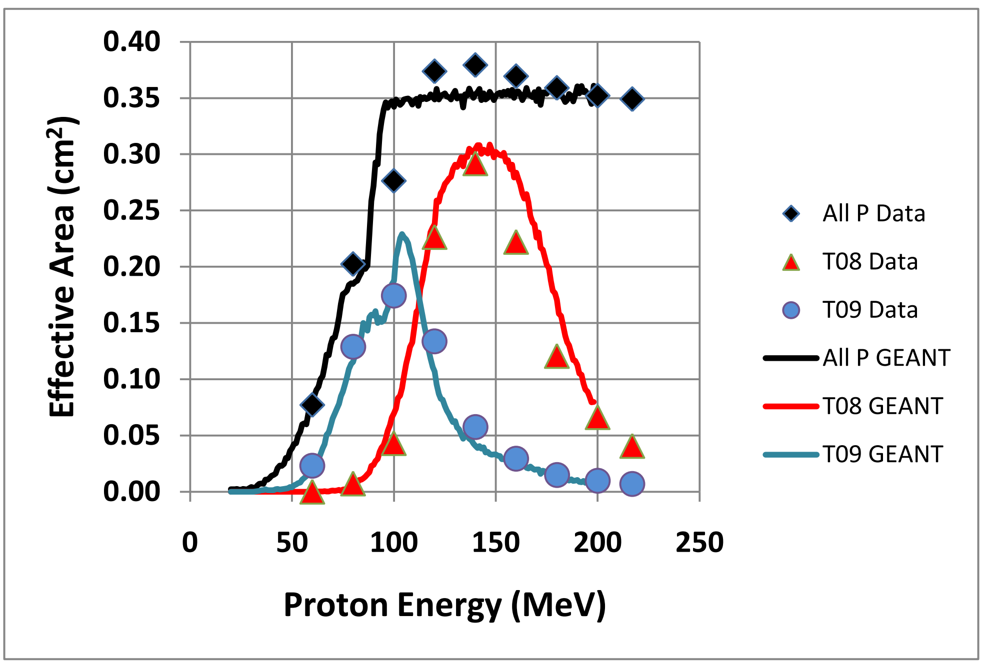

Figure 6 Comparison of Measured Effective 0^o Areas to Results of GEANT Calculations

Table 4 S/N 004 Angular Response at 60 MeV

Angle (deg)	All Protons (cm^2)	T05 (cm^2)	T06 (cm^2)	T08 (cm^2)	T09 (cm^2)
0	0.077	0.020	0.029	0.000	0.023
10	0.067	0.016	0.027	0.000	0.021
20	0.042	0.008	0.017	0.000	0.014
30	0.013	0.002	0.006	0.000	0.005
40	0.000	0.000	0.000	0.000	0.000
50	0.000	0.000	0.000	0.000	0.000
60	0.000	0.000	0.000	0.000	0.000

Table 5 S/N 004 Angular Response at 80 MeV

Angle (deg)	All Protons (cm^2)	T05 (cm^2)	T06 (cm^2)	T08 (cm^2)	T09 (cm^2)
0	0.202	0.014	0.051	0.007	0.129
10	0.190	0.018	0.065	0.006	0.100
20	0.166	0.040	0.060	0.003	0.060
30	0.084	0.041	0.013	0.019	0.000
40	0.008	0.004	0.001	0.000	0.000
50	0.000	0.000	0.000	0.000	0.000
60	0.000	0.000	0.000	0.000	0.000

Table 6 S/N 004 Angular Response at 100 MeV

Angle (deg)	All Protons (cm^2)	T05 (cm^2)	T06 (cm^2)	T08 (cm^2)	T09 (cm^2)
0	0.276	0.005	0.053	0.043	0.174
10	0.269	0.006	0.058	0.037	0.167
20	0.232	0.010	0.064	0.020	0.136
30	0.134	0.002	0.053	0.004	0.073
40	0.065	0.014	0.030	0.000	0.018
50	0.010	0.004	0.004	0.000	0.001
60	0.001	0.001	0.000	0.000	0.000

Table 7 S/N 004 Angular Response at 120 MeV

Angle (deg)	All Protons (cm^2)	T05 (cm^2)	T06 (cm^2)	T08 (cm^2)	T09 (cm^2)
0	0.374	0.001	0.011	0.227	0.134
10	0.363	0.001	0.011	0.211	0.139
20	0.332	0.001	0.012	0.151	0.164
30	0.265	0.002	0.012	0.053	0.192
40	0.173	0.006	0.037	0.004	0.121
50	0.071	0.018	0.032	0.002	0.017
60	0.027	0.013	0.010	0.002	0.000

Table 8 S/N 004 Angular Response at 140 MeV

Angle (deg)	All Protons (cm^2)	T05 (cm^2)	T06 (cm^2)	T08 (cm^2)	T09 (cm^2)
0	0.379	0.000	0.002	0.292	0.057
10	0.374	0.000	0.002	0.291	0.061
20	0.329	0.000	0.002	0.246	0.067
30	0.273	0.001	0.004	0.171	0.088
40	0.181	0.001	0.005	0.056	0.111
50	0.120	0.001	0.011	0.006	0.097
60	0.037	0.001	0.006	0.001	0.026

Table 9 S/N 004 Angular Response at 160 MeV

Angle (deg)	All Protons (cm^2)	T05 (cm^2)	T06 (cm^2)	T08 (cm^2)	T09 (cm^2)
0	0.369	0.000	0.001	0.222	0.029
10	0.365	0.000	0.001	0.236	0.031
20	0.340	0.000	0.001	0.247	0.038
30	0.261	0.000	0.001	0.197	0.045
40	0.183	0.000	0.002	0.106	0.065
50	0.092	0.000	0.002	0.017	0.067
60	0.033	0.000	0.001	0.003	0.025

Table 10 S/N 004 Angular Response at 180 MeV

Angle (deg)	All Protons (cm^2)	T05 (cm^2)	T06 (cm^2)	T08 (cm^2)	T09 (cm^2)
0	0.359	0.000	0.001	0.121	0.015
10	0.352	0.000	0.001	0.134	0.016
20	0.318	0.000	0.001	0.157	0.019
30	0.261	0.000	0.001	0.179	0.027
40	0.188	0.000	0.001	0.134	0.038
50	0.096	0.000	0.001	0.042	0.045
60	0.032	0.000	0.001	0.006	0.020

Table 11 S/N 004 Angular Response at 200 MeV

Angle (deg)	All Protons (cm^2)	T05 (cm^2)	T06 (cm^2)	T08 (cm^2)	T09 (cm^2)
0	0.352	0.000	0.001	0.066	0.010
10	0.334	0.000	0.001	0.072	0.010
20	0.318	0.000	0.001	0.094	0.012
30	0.259	0.000	0.001	0.128	0.017
40	0.185	0.000	0.001	0.131	0.024
50	0.096	0.000	0.001	0.057	0.028
60	0.023	0.000	0.001	0.002	0.014

Table 12 S/N 004 Angular Response at 217 MeV

Angle (deg)	All Protons (cm^2)	T05 (cm^2)	T06 (cm^2)	T08 (cm^2)	T09 (cm^2)
0	0.349	0.000	0.001	0.041	0.007
10	0.336	0.000	0.001	0.045	0.007
20	0.300	0.000	0.001	0.055	0.008
30	0.237	0.000	0.001	0.082	0.011
40	0.180	0.000	0.001	0.111	0.017
50	0.096	0.000	0.001	0.063	0.020
60	0.000	0.000	0.000	0.000	0.000

4.2 Calibration for CEASE S/N 006

Since the top material (Cu) for S/N 006 is less dense than the material (W) for S/N 004, the response of this unit shifts to lower energies relative to S/N 004. Effective 0^o areas for the Tn channels were computed using eq. (6) (see Table 13) and are plotted in Figure 7. The “All P” channel contains the sum of all CEASE particles not identified as electrons. The total effective area peaks at 0.421 cm^2 at 120 and 140 MeV. For energies above 140 MeV, proton counts begin to move out of the proton identification region into the electron region and effective area of the "All Protons" and sum of the Tn channels decreases with increasing proton energy.

Table 13 Effective Areas for CEASE S/N006 at Normal Incidence

Energy (MeV)	All Protons (cm^2)	T05 (cm^2)	T06 (cm^2)	T08 (cm^2)	T09 (cm^2)	Sum Tn (cm^2)
40	0.137	0.060	0.065	0.000	0.000	0.125
60	0.245	0.008	0.056	0.001	0.180	0.244
80	0.411	0.002	0.041	0.070	0.298	0.411
100	0.407	0.001	0.017	0.230	0.158	0.406
120	0.421	0.002	0.004	0.312	0.093	0.411
140	0.421	0.000	0.002	0.273	0.055	0.330
160	0.410	0.000	0.002	0.174	0.035	0.211
200	0.375	0.000	0.001	0.064	0.018	0.084

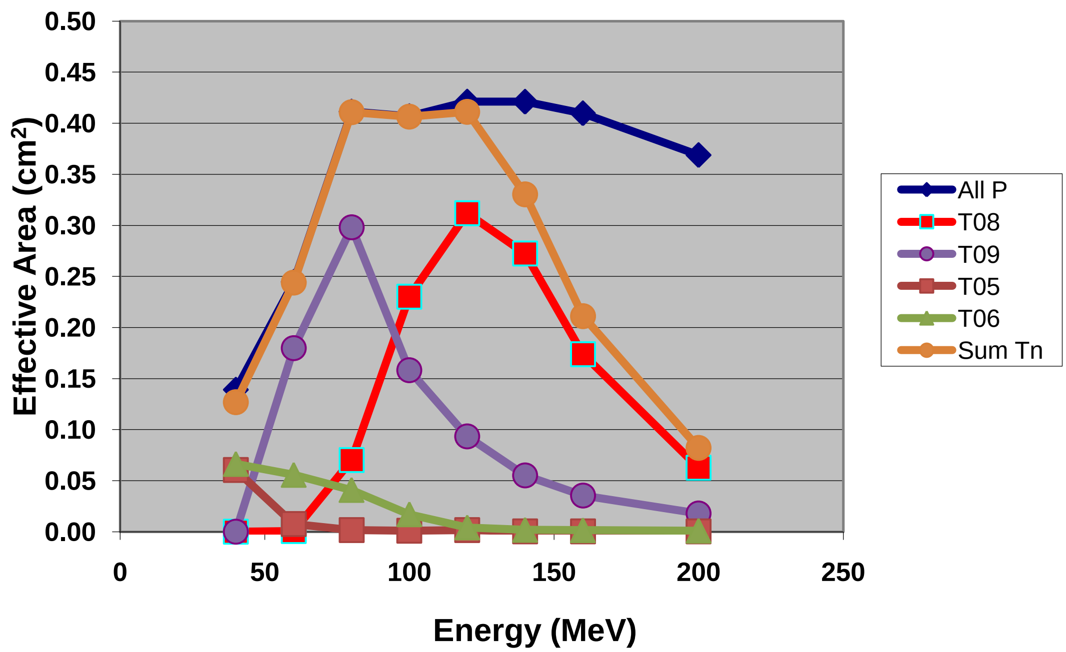

Figure 7 Effective Areas of S/N 006 Channels as a Function of Energy

The geometric factors for S/N 006 T0n channels are listed in Table 14 and are plotted in Figure 8.

Table 14 Geometric Factors for the CEASE S/N 006 T0n Channels

E (MeV)	All Protons cm^2-sr	T05 cm^2-sr	T06 cm^2-sr	T08 cm^2-sr	T09 cm^2-sr	Sum Tn cm^2-sr
40	0.092	0.037	0.047	0.000	0.002	0.086
60	0.190	0.019	0.065	0.000	0.101	0.185
80	0.401	0.027	0.122	0.028	0.218	0.395
100	0.516	0.032	0.094	0.109	0.272	0.507
120	0.682	0.003	0.037	0.264	0.303	0.607
140	0.654	0.001	0.013	0.352	0.230	0.596
160	0.658	0.001	0.008	0.359	0.166	0.534
200	0.578	0.001	0.003	0.242	0.075	0.321

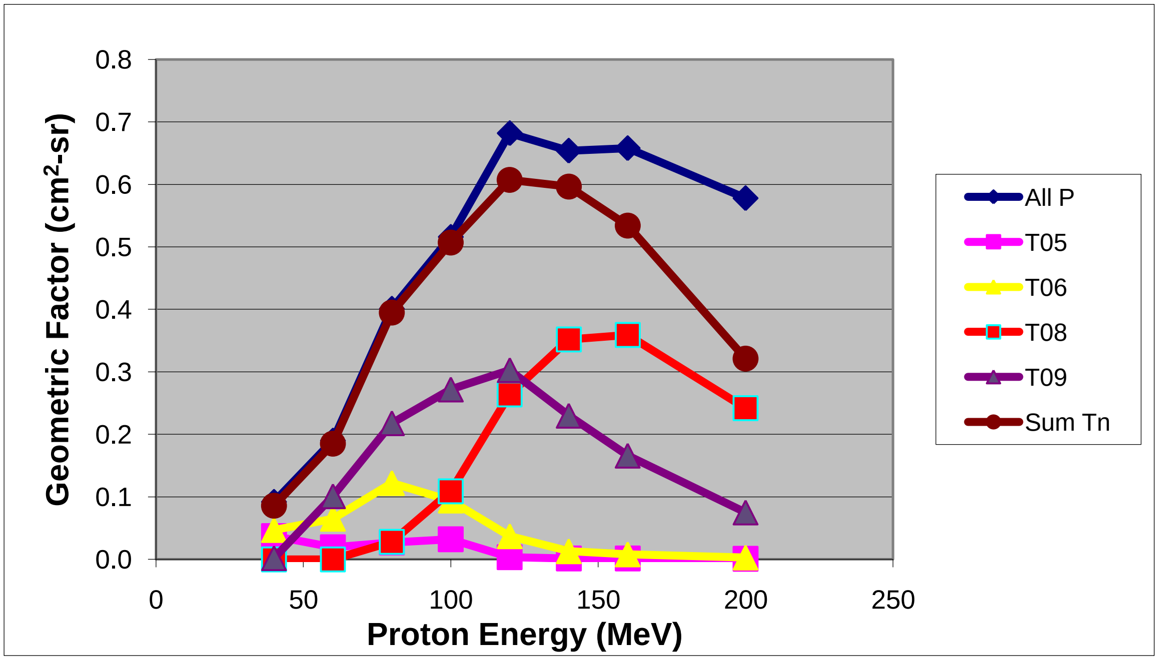

Figure 8 Geometric Factors for the CEASE S/N 006 T0n Channels

The angular responses as a function of energy for the T0n channels of S/N006 are listed in Tables 15 through 22.

Table 15 S/N 006 Angular Response at 40 MeV

Angle	**All Protons**	**T05**	**T06**	**T08**	**T09**
(deg)	(cm^2)	(cm^2)	(cm^2)	(cm^2)	(cm^2)
0	0.139	0.061	0.066	0.000	0.000
10	0.132	0.054	0.064	0.000	0.004
20	0.091	0.035	0.048	0.000	0.001
30	0.045	0.017	0.024	0.000	0.000
40	0.009	0.004	0.003	0.000	0.001
50	0.000	0.000	0.000	0.000	0.000

Table 16 S/N 006 Angular Response at 60 MeV

Angle	**All Protons**	**T05**	**T06**	**T08**	**T09**
(deg)	(cm^2)	(cm^2)	(cm^2)	(cm^2)	(cm^2)
0	0.240	0.007	0.055	0.001	0.177
10	0.229	0.011	0.057	0.000	0.159
20	0.178	0.016	0.061	0.000	0.097
30	0.114	0.015	0.048	0.000	0.048
40	0.018	0.003	0.006	0.000	0.007
50	0.000	0.000	0.000	0.000	0.000

Table 17 S/N 006 Angular Response at 80 MeV

Angle (deg)	**All Protons (cm^2)**	**T05 (cm^2)**	**T06 (cm^2)**	**T08 (cm^2)**	**T09 (cm^2)**
0	0.404	0.002	0.040	0.069	0.293
5	0.401	0.002	0.045	0.067	0.287
10	0.393	0.002	0.060	0.058	0.273
20	0.353	0.003	0.100	0.031	0.217
30	0.247	0.012	0.097	0.007	0.127
40	0.110	0.033	0.052	0.000	0.020
50	0.009	0.006	0.002	0.000	0.000

Table 18 S/N 006 Angular Response at 100 MeV

Angle (deg)	All Protons (cm^2)	T05 (cm^2)	T06 (cm^2)	T08 (cm^2)	T09 (cm^2)
0	0.393	0.001	0.017	0.223	0.153
10	0.390	0.001	0.018	0.208	0.163
20	0.238	0.001	0.014	0.094	0.127
30	0.279	0.002	0.025	0.051	0.196
40	0.181	0.007	0.056	0.003	0.109
50	0.072	0.026	0.035	0.000	0.010

19 S/N 006 Angular Response at 120 MeV

Angle (deg)	All Protons (cm^2)	T05 (cm^2)	T06 (cm^2)	T08 (cm^2)	T09 (cm^2)
0	0.421	0.000	0.004	0.312	0.093
10	0.414	0.000	0.004	0.304	0.097
20	0.379	0.000	0.005	0.255	0.110
30	0.298	0.001	0.008	0.151	0.129
40	0.202	0.001	0.013	0.030	0.150
50	0.103	0.002	0.022	0.002	0.072

Table 20 S/N 006 Angular Response at 140 MeV

Angle (deg)	All Protons (cm^2)	T05 (cm^2)	T06 (cm^2)	T08 (cm^2)	T09 (cm^2)
0	0.421	0.000	0.002	0.273	0.055
10	0.430	0.000	0.002	0.292	0.060
20	0.384	0.000	0.002	0.274	0.066
30	0.306	0.000	0.003	0.211	0.076
40	0.208	0.000	0.005	0.095	0.097
50	0.116	0.001	0.007	0.009	0.089

Table 21 S/N 006 Angular Response at 160 MeV

Angle (deg)	All Protons (cm^2)	T05 (cm^2)	T06 (cm^2)	T08 (cm^2)	T09 (cm^2)
0	0.410	0.000	0.002	0.174	0.035
10	0.428	0.000	0.002	0.199	0.040
20	0.380	0.000	0.002	0.216	0.044
30	0.309	0.000	0.002	0.214	0.052
40	0.215	0.000	0.003	0.133	0.065
50	0.115	0.000	0.004	0.030	0.072

Table 22 S/N 006 Angular Response at 200 MeV

Angle (deg)	All Protons (cm^2)	T05 (cm^2)	T06 (cm^2)	T08 (cm^2)	T0-9 (cm^2)
0	0.369	0.000	0.001	0.063	0.018
10	0.360	0.000	0.001	0.067	0.019
20	0.327	0.000	0.001	0.079	0.021
30	0.267	0.000	0.001	0.103	0.023
40	0.195	0.000	0.001	0.123	0.030
50	0.106	0.000	0.001	0.061	0.031

5. SUMMARY

A series of calibrations of two CEASE units was carried out at the high energy proton cyclotron at Massachusetts General Hospital in February and June of 2009. One CEASE unit, S/N 004 is a flight unit with a modified tungsten collimator; S/N 006 is an engineering model identical to the CEASE unit flown on the TSX-5 mission. A detailed listing of the measured effective 0^o areas, geometric factors, and angular response for two CEASE units has been presented in tables. The measured effective 0^o areas and the results of GEANT calculations are in good agreement. The listed geometric factors can be used to convert the on-orbit CEASE counts to particle flux in physical units.

REFERENCES

[1] Dichter, B, McGarity, J., Golightly, M., Brautigam, D. and Woolf, S., “Calibration Report for the Particle Telescope on the Compact Environmental Anomaly Sensor (CEASE),” AFRL-VS-HA-TR-2006-1098, Assurance Technology Corporation, 84 South Street, Carlisle, MA 01741-1515, 8-09-06.
.

[2] Brautigam, D., “Compact Environmental Anomaly Sensor (CEASE): Geometric Factors,” AFRL-RV-HA-TR-2008-1129, Air Force Research Laboratory, 29 Randolph Rd., Hanscom AFB, MA 01731-3010, 11-4-08.

DISTRIBUTION LIST

DTIC/OCP 8725 John J. Kingman Rd, Suite 0944 Ft Belvoir, VA 22060-6218	1 cy
AFRL/RVIL Kirtland AFB, NM 87117-5776	2 cys
Official Record Copy AFRL/RVBXR/Chadwick Lindstrom	1 cy